Effect of Intrinsic Defects in High-Purity Semi-Insulating 4H-SiC on Reverse Current–Voltage Characteristics of Schottky Barrier Diodes

Hideharu Matsuura*, Yoshitaka Kagawa, Miyuki Takahashi, Shoichi Tano, and Takayuki Miyake

Department of Electronic Engineering and Computer Science, Osaka Electro-Communication University, 18-8 Hatsu-cho, Neyagawa, Osaka 572-8530, Japan

Received October 4, 2008; accepted February 16, 2009; published online May 20, 2009

Schottky barrier diodes are fabricated using high-purity semi-insulating 4H-SiC. Under certain measurement conditions, the reverse current–voltage (I_R–V) characteristics of the diodes exhibit a peak, with the diodes appearing to behave as negative resistance diodes. To investigate the effect of intrinsic defects in the 4H-SiC on the I_R–V characteristics, the transient reverse currents of the diodes are measured. Without any assumptions regarding defects, a graphical peak analysis method, discharge current transient spectroscopy (DCTS), which uses the isothermal transient reverse current, can determine the densities and emission rates of defects. From simulation of the I_R–V characteristics using the densities and emission rates of intrinsic defects determined by DCTS, the effect of the intrinsic defects in high-purity semi-insulating 4H-SiC on the I_R–V characteristics of its Schottky barrier diodes is elucidated. It is found that DCTS is suitable for determining the densities and emission rates of electrically active defects in semi-insulating semiconductors.
© 2009 The Japan Society of Applied Physics

DOI: 10.1143/JJAP.48.056504

1. Introduction

High-purity Si pin diodes, Li-doped Si Schottky barrier diodes, and high-purity Ge pin diodes have been developed for use in X-ray energy spectroscopy.[1,2] To form a wide depletion region in the diode, a high reverse bias (e.g., 100 V) must be applied to the diode. Since the resistivity of high-purity Si or Ge is not sufficiently high to reduce the reverse current of the diode to 1 nA at room temperature under the high reverse bias condition, highly resistive HgI_2 and CdTe have been investigated as alternatives.[1,2] In recent studies, highly purified SiC was formed, and its resistivity was found to be much higher than 10^6 Ω cm.[3–5]

When a high reverse bias is applied to the diode, a transient reverse current flows, which may break the junction field-effect transistor connected to the diode.[6,7] The transient reverse current is related to electrically active intrinsic defects (i.e., traps). Because traps behave as generation centers in the depletion region of the diode and produce a generation current in the reverse-biased diode, they degrade the performance of X-ray detectors. To determine the possibility of high-purity semi-insulating SiC being used as a portable X-ray detector operating at room temperature or elevated temperatures,[8] it is necessary to investigate traps related to the transient reverse current.

Although powerful methods to characterize traps in low-resistivity semiconductors are transient capacitance methods, e.g., deep level transient spectroscopy,[9] these are not feasible in semi-insulating semiconductors because the measured capacitance of the diode fabricated using semi-insulating semiconductors is determined by the thickness of the diode, not by the depletion region of the junction.[10–14] Thermally stimulated current (TSC)[15] is suitable for characterizing traps in semi-insulating semiconductors. However, it is difficult to analyze experimental TSC data when traps with similar emission rates are included in the semiconductor. Moreover, because the effect of pyroelectric currents and the temperature dependence of the steady-state leakage current must be considered in the TSC analysis, an isothermal measurement is more suitable for characterizing traps than TSC is.

Without making any assumptions regarding the traps, one of the authors has proposed a graphical peak analysis method, referred to as discharge current transient spectroscopy (DCTS),[16–20] for determining the densities and emission rates of traps using the isothermally measured transient reverse current, and has applied it to SiN_x films,[16,17] $Pb(Zr,Ti)O_3$ films,[18] and high-resistivity Si (i-layer) in pin diodes.[19,20] From each peak of the DCTS signal, the density and emission rate of the corresponding trap can be determined accurately.

In this paper, we report on the effect of traps in high-purity semi-insulating 4H-SiC on the reverse current–voltage (I_R–V) characteristics of its Schottky barrier diodes, where the densities and emission rates of the traps are determined by DCTS.

2. Experimental Methods

A 0.37-mm-thick high-purity semi-insulating on-axis 4H-SiC wafer, which was polished on both sides and guaranteed to be ready for epitaxial growth, was purchased from Cree. After native oxide layers on the samples were removed using HF, Ni electrodes with a radius of 1.25 mm were evaporated in vacuum onto both sides of the samples. Since thermal treatment was not carried out, the diodes worked as a back-to-back diode.[8] The I_R–V characteristics of the diodes were measured from 0 to 100 V by an increment of reverse bias (ΔV_R) using a Keithley 236 source-measure unit (SMU236). ΔV_R was selected to be 1 V. In the I_R–V measurements, we waited for a certain period of time (Δt) to measure the reverse current at each reverse bias after the bias was increased by ΔV_R. DCTS measurements were performed at a reverse bias (V_R) of 100 V at 373 K using the SMU236.

3. Results and Discussion

Figure 1 shows the I_R–V characteristics for a Δt of 1 s at 303 and 373 K, denoted by △ and ○, respectively. At both measurement temperatures, one peak appeared at a reverse bias lower than 10 V, which seemed to indicate that the diode was working as a negative resistance diode.

To investigate the origin of this unusual behavior, the effect of the traps in the high-purity semi-insulating 4H-SiC on the I_R–V characteristics is evaluated. Figure 2 shows the

*E-mail address: matsuura@isc.osakac.ac.jp

 © 2009 The Japan Society of Applied Physics

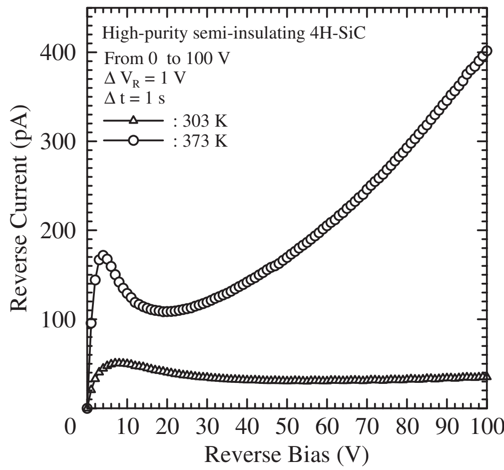

Fig. 1. I_R–V characteristics for a Δt of 1 s at 303 and 373 K.

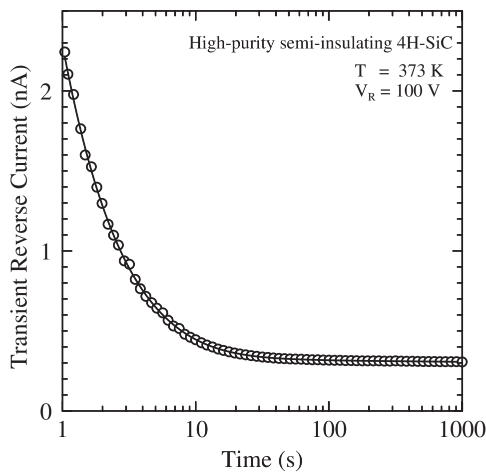

Fig. 2. Transient reverse current at 373 K.

transient reverse current $i_R(t)$ at 373 K after a V_R of 100 V is applied to a diode held at thermal equilibrium (0 V) for 5 min. In the figure, ○ represents the experimental $i_R(t)$, and the solid line is calculated by interpolating the experimental $i_R(t)$ with a cubic smoothing natural spline function. When the emission of the charged carriers from traps in the depletion region of the diode affects $i_R(t)$, the properties of the traps related to the $i_R(t)$ can be investigated using DCTS.

Using the experimental $i_R(t)$, the DCTS signal $D(t, e_{ref})$ is defined as[8,18–20)]

$$D(t, e_{ref}) \equiv \frac{t}{qS}[i_R(t) - I_R(V_R)]\exp(-e_{ref}t + 1), \quad (1)$$

where q is the electron charge, S is the electrode area, $I_R(V_R)$ is the steady-state reverse current at V_R, and e_{ref} is the peak-shift parameter. The DCTS signal has a peak corresponding to each trap. From each peak of the DCTS signal, the sheet density (N_{Ti}) and emission rate (e_{Ti}) of the ith trap can be independently determined as[8,18–20)]

$$e_{Ti} = \frac{1}{t_{peaki}} - e_{ref} \quad (2)$$

and

$$N_{Ti} = \frac{D(t_{peaki}, e_{ref})}{1 - e_{ref}t_{peaki}}. \quad (3)$$

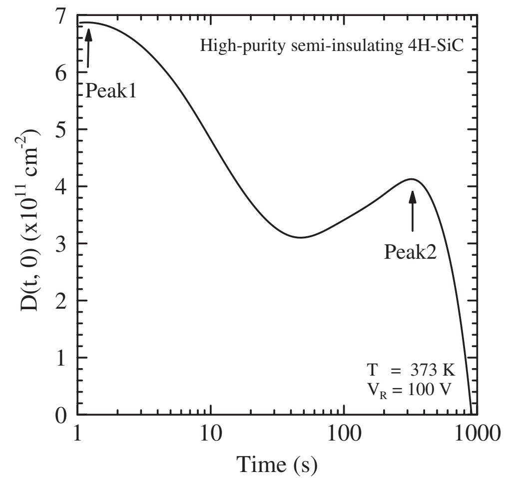

Fig. 3. DCTS signal at 373 K.

This calculation is probable because $i_R(t)$ is theoretically given by[8,18–20)]

$$i_R(t) = qS\sum_i N_{Ti}e_{Ti}\exp(-e_{Ti}t) + I_R(V_R). \quad (4)$$

Traps determined by DCTS are located both at the interface and in the bulk.

Figure 3 shows $D(t, e_{ref})$ calculated with an e_{ref} of $0\,s^{-1}$ using eq. (1). In Fig. 3, there are two peaks labeled Peak1 and Peak2. From t_{Peak1} and $D(t_{Peak1}, 0)$, the values of N_{T1} and e_{T1} for Trap1 are determined to be $6.9 \times 10^{11}\,cm^{-2}$ and $8.6 \times 10^{-1}\,s^{-1}$, respectively, while from t_{Peak2} and $D(t_{Peak2}, 0)$, N_{T2} and e_{T2} for Trap2 are determined to be $4.1 \times 10^{11}\,cm^{-2}$ and $3.1 \times 10^{-3}\,s^{-1}$, respectively. This analysis was carried out using software developed in-house.[21)]

Let us consider the transient reverse current in detail. In the following discussion, it is assumed that the traps determined by DCTS uniformly exist in the bulk. The width of the depletion layer $W(V_{Rj})$ at the jth reverse bias (V_{Rj}) is given by

$$W(V_{Rj}) = A\sqrt{V_d + V_{Rj}} \quad (5)$$

and

$$V_{Rj} = \Delta V_R \times j \quad (j = 0, 1, \ldots, n), \quad (6)$$

where V_d is the diffusion potential for the Schottky barrier junction and A is a proportionality constant. N_{Ti} is the total charge per unit area of the charged carriers trapped at the ith trap in thermal equilibrium over the width (W_{total}) given by

$$W_{total} = A(\sqrt{V_d + V_{Rn}} - \sqrt{V_d + V_{R0}}). \quad (7)$$

Since $V_{Rn} = 100$ V and $\Delta V_R = 1$ V in this experiment, n is 100.

By changing V_{Rj-1} to V_{Rj}, the increment of the depletion layer is described as

$$\Delta W(V_{Rj}) = W(V_{Rj}) - W(V_{Rj-1}). \quad (8)$$

When it is a neutral layer, $\Delta W(V_{Vj})$ includes the charge $\Delta Q_{Ti}(V_{Rj})$ of charged carriers trapped at the ith trap. Therefore, $\Delta Q_{Ti}(V_{Rj})$ is given by

© 2009 The Japan Society of Applied Physics

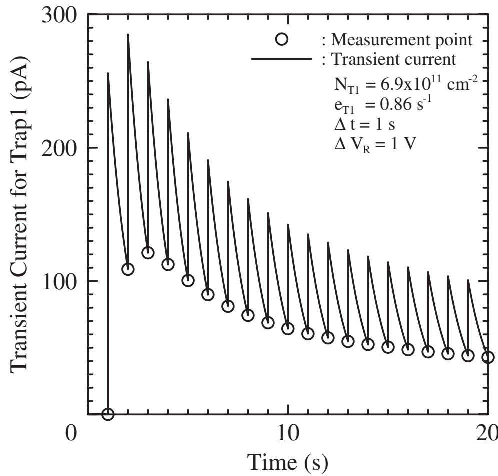

Fig. 4. Simulation of measurement points and transient current for Trap1 during the I_R–V measurement.

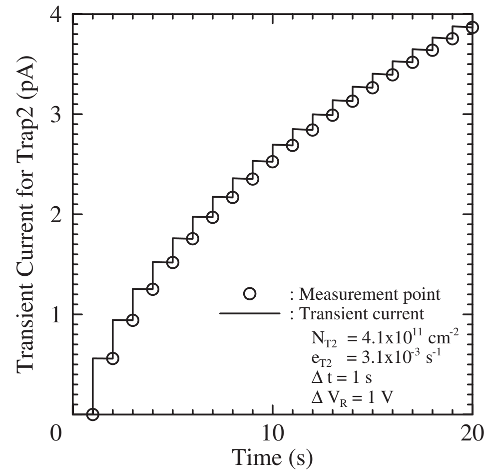

Fig. 5. Simulation of measurement points and transient current for Trap2 during I_R–V measurement.

$$\Delta Q_{\mathrm{T}i}(V_{\mathrm{R}j}) = SN_{\mathrm{T}i}\frac{\Delta W(V_{\mathrm{R}j})}{W_{\mathrm{total}}} = SN_{\mathrm{T}i}\frac{\sqrt{V_{\mathrm{d}}+V_{\mathrm{R}j}}-\sqrt{V_{\mathrm{d}}+V_{\mathrm{R}j-1}}}{\sqrt{V_{\mathrm{d}}+V_{\mathrm{R}n}}-\sqrt{V_{\mathrm{d}}+V_{\mathrm{R0}}}} \quad (j = 1, 2, \ldots, n) \tag{9}$$

and $\Delta Q_{\mathrm{T}i}(V_{\mathrm{R0}}) = 0$. On the basis of eq. (4), the component $i_i(t)$ of the transient current for the ith trap, which does not include the steady-state reverse current, is theoretically derived as

$$i_i(t) = q\sum_{j=0}^{n}\Delta Q_{\mathrm{T}i}(V_{\mathrm{R}j})e_{\mathrm{T}i}f(t - t_j), \tag{10}$$

where

$$f(t - t_j) = \begin{cases} \exp[-e_{\mathrm{T}i}(t - t_j)] & t \geq t_j \\ 0 & t < t_j \end{cases} \tag{11}$$

and

$$t_j = \Delta t \times j. \tag{12}$$

In Fig. 4, the solid line represents $i_1(t)$ simulated with a Δt of 1 s, an N_{T1} of 6.9×10^{11} cm^{-1} and an e_{T1} of 0.86 s^{-1}, and open circles represent the measurement points. Here, V_{d} was assumed to be 0.5 V. The transient current increases when the reverse bias is increased by ΔV_{R}, and then exponentially decreases. When Δt passes, the reverse current is measured, which is denoted by ○ in Fig. 4. Since $1/e_{\mathrm{T1}}$ is close to a Δt of 1 s, the transient current at $V_{\mathrm{R}j}$ decreases by approximately one-half during Δt. $\Delta Q_{\mathrm{T1}}(V_{\mathrm{R}j})$ decreases with increasing $V_{\mathrm{R}j}$. Finally, the measurement reverse current shown by ○ in Fig. 4 initially increases and then decreases with increasing reverse bias. When the component for Trap1 is dominant, the I_{R}–V characteristics must have a peak.

In Fig. 5, the solid line represents $i_2(t)$ simulated with a Δt of 1 s, an N_{T2} of 4.1×10^{11} cm^{-2} and an e_{T2} of 3.1×10^{-3} s^{-1}, and open circles represents the measurement points. Since $1/e_{\mathrm{T2}}$ is much longer than a Δt of 1 s, the transient current at $V_{\mathrm{R}j}$ is nearly constant during Δt. Finally, the measurement reverse current shown by ○ in Fig. 5 increases monotonically with increasing reverse bias.

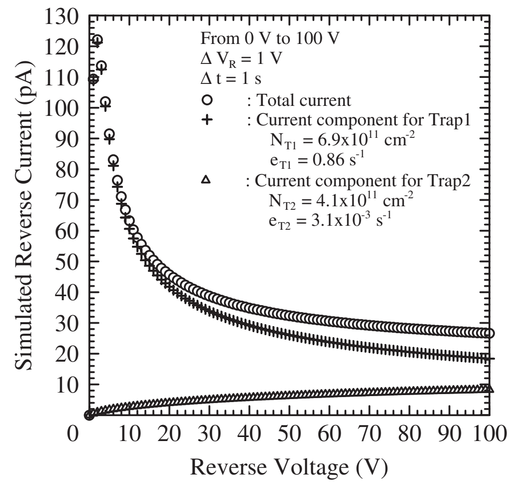

Fig. 6. Simulation of I_R–V characteristics due to Trap1 and Trap2.

Figure 6 shows the simulated I_{R}–V characteristics (○) due to both Trap1 and Trap2, and the simulated components for Trap1 (+) and Trap2 (△). The steady-state reverse current is not included here. The unusual I_{R}–V characteristics result from the component of the reverse current for Trap1.

To eliminate the effect of Trap1 from the experimental I_{R}–V characteristics, it is necessary to make Δt longer. When Δt is longer than $1/e_{\mathrm{T1}}$ by approximately 10, for example, the effect of the transient current due to Trap1 on the experimental reverse current must be negligible. Figure 7 shows the experimental I_{R}–V characteristics corresponding to Δt values of 1 and 10 s, indicated by ○ and ●, respectively. As can be seen from the figure, I_{R}–V characteristics not affected by Trap1 are obtained when $\Delta t = 10$ s. Furthermore, the simulated component of the reverse current due to Trap2 is lower than 10 pA at 100 V in Fig. 6, which is much less than the experimental reverse current at 100 V for a Δt of 10 s. Therefore, the I_{R}–V characteristics for a Δt of 10 s are close to the steady-state I_{R}–V characteristics. It is worth mentioning that Δt should be carefully chosen when the I_{R}–V characteristics in diodes fabricated using semi-insulating semiconductors are measured.

© 2009 The Japan Society of Applied Physics

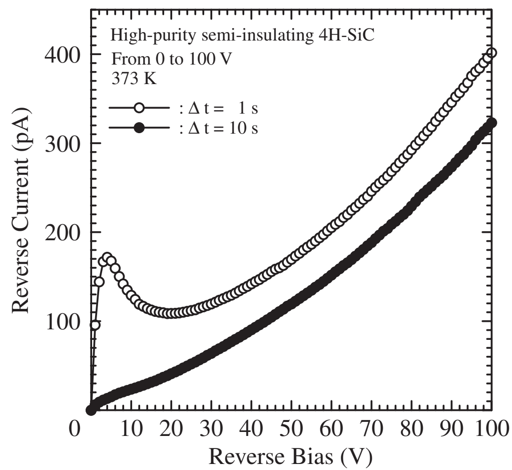

Fig. 7. I_R–V characteristics for delay times of 1 and 10 s.

4. Conclusions

The I_R–V characteristics of Schottky barrier diodes formed using high-purity semi-insulating 4H-SiC were experimentally and theoretically investigated. The effect of electrically active defects in the 4H-SiC on the I_R–V characteristics was discussed. When the reverse bias is increased, a transient current flows. This is because charged carriers trapped at defects in the depletion region are emitted when the neutral region is changed into the depletion region owing to the increase in the reverse bias. Unless the transient current vanishes for a period of time between applying the reverse bias and measuring the reverse current, the measured I_R–V characteristics are strongly affected by the defects. The densities and emission rates of defects in 4H-SiC were determined by DCTS. The I_R–V characteristics simulated using the obtained values of densities and emission rates were similar to the experimental I_R–V characteristics. Thus, the I_R–V characteristics of diodes fabricated using semi-insulating semiconductors must be measured for an adequate period of time. Moreover, it is found that DCTS can be used to determine the densities and emission rates of defects in semi-insulating semiconductors.

Acknowledgments

This work was partially supported by the Academic Frontier Promotion Projects of the Ministry of Education, Culture, Sports, Science and Technology of Japan in 2003–2007 and by a Grant-in-Aid for Scientific Research (C) from the Japan Society for the Promotion of Science in 2006 and 2007 (18560356).

1) G. Lutz: *Semiconductor Radiation Detectors* (Springer, Berlin, 1999) p. 79.
2) H. Spieler: *Semiconductor Detector Systems* (Oxford University Press, Oxford, U.K., 2005) p. 83.
3) J. R. Jenny, St. G. Müller, A. R. Powell, V. F. Tsvetkov, H. M. Hobgood, R. C. Glass, and C. H. Carter, Jr.: J. Electron. Mater. **31** (2002) 366.
4) J. R. Jenny, D. P. Malta, M. R. Calus, St. G. Müller, A. R. Powell, V. F. Tsvetkov, H. M. Hobgood, R. C. Glass, and C. H. Carter, Jr.: Mater. Sci. Forum **457–460** (2004) 35.
5) H. Matsuura, H. Yanase, and M. Takahashi: Jpn. J. Appl. Phys. **47** (2008) 7052.
6) H. Matsuura and K. Nishida: Jpn. J. Appl. Phys. **37** (1998) L115.
7) H. Matsuura, K. Akatani, M. Ueda, K. Segawa, H. Tomozawa, K. Nishida, and K. Taniguchi: Jpn. J. Appl. Phys. **38** (1999) L1015.
8) H. Matsuura, M. Takahashi, S. Nagata, and K. Taniguchi: J. Mater. Sci.: Mater. Electron. **19** (2008) 810.
9) D. V. Lang: J. Appl. Phys. **45** (1974) 3023.
10) H. Matsuura, T. Okuno, H. Okushi, and K. Tanaka: J. Appl. Phys. **55** (1984) 1012.
11) H. Matsuura: J. Appl. Phys. **64** (1988) 1964.
12) H. Matsuura: IEEE Trans. Electron Devices **36** (1989) 2908.
13) H. Matsuura: J. Appl. Phys. **68** (1990) 1138.
14) H. Matsuura, N. Minohara, and T. Ohshima: J. Appl. Phys. **104** (2008) 043702.
15) R. R. Haering and E. N. Adams: Phys. Rev. **117** (1960) 451.
16) H. Matsuura, M. Yoshimoto, and H. Matsunami: Jpn. J. Appl. Phys. **34** (1995) L185.
17) H. Matsuura, M. Yoshimoto, and H. Matsunami: Jpn. J. Appl. Phys. **34** (1995) L371.
18) H. Matsuura, T. Hase, Y. Sekimoto, M. Uchida, and M. Shimizu: J. Appl. Phys. **91** (2002) 2085.
19) H. Matsuura and K. Segawa: Jpn. J. Appl. Phys. **39** (2000) 178.
20) H. Matsuura, K. Segawa, and T. Ebisui: Jpn. J. Appl. Phys. **39** (2000) 2714.
21) The application software for DCTS for the Windows operating system can be downloaded for free at our web site [http://www.osakac.ac.jp/labs/matsuura/].

© 2009 The Japan Society of Applied Physics